Advances in Water Resources 34 (2011) 495–504

Contents lists available at ScienceDirect

Advances in Water Resources

journal homepage: www.elsevier.com/locate/advwatres

Effect of streamflow forecast uncertainty on real-time reservoir operation

Tongtiegang Zhao [a,b], Ximing Cai [b,*], Dawen Yang [a]

[a] Institute of Hydrology and Water Resources, Department of Hydraulic Engineering, Tsinghua University, Beijing, China
[b] Ven Te Chow Hydrosystem Laboratory, Department of Civil and Environmental Engineering, University of Illinois at Urbana Champaign, Champaign, IL 61801, USA

ARTICLE INFO

Article history:
Received 3 September 2010
Received in revised form 3 January 2011
Accepted 10 January 2011
Available online 13 January 2011

Keywords:
Streamflow forecast uncertainty
Real-time reservoir operation
Deterministic streamflow forecast
Probabilistic streamflow forecast
Martingale Model of Forecast Evolution

ABSTRACT

Various hydrological forecast products have been applied to real-time reservoir operation, including deterministic streamflow forecast (*DSF*), *DSF*-based probabilistic streamflow forecast (*pseudo-PSF, pPSF*), and ensemble or probabilistic streamflow forecast (denoted as *real-PSF, rPSF*). *DSF* represents forecast uncertainty in the form of deterministic forecast errors, *pPSF* a conditional distribution of forecast uncertainty for a given *DSF*, and *rPSF* a probabilistic uncertainty distribution. Compared to previous studies that treat the forecast products as *ad hoc* inputs for reservoir operation models, this paper attempts to model the dynamic evolution of uncertainties involved in the various forecast products and explores their effect on real-time reservoir operation decisions. Through a hypothetical example of a single-objective real-time reservoir operation model, the results illustrate that forecast uncertainty exerts significant effects. Reservoir operation efficiency, as measured by a utility function, decreases as the forecast uncertainty increases but the magnitude depends on the forecast products used. In general, the utility of the reservoir operation with *rPSF* is nearly as high as the utility obtained with a perfect forecast. Meanwhile, the utilities of *DSF* and *pPSF* are similar to each other but not as high as *rPSF*. Moreover, streamflow variability and reservoir capacity can change the magnitude of the effects of forecast uncertainty, but not the relative merit of *DSF*, *pPSF*, and *rPSF*.

1. Introduction

Advances in weather forecasting, hydrologic modeling, and hydro-climatic teleconnection relationships have significantly improved streamflow forecast precision and lead-time [3,22,24,28] and provide great opportunities to improve the efficiency of water resources system operations [23,25,29,39]. In recent years, forecast products, particularly long-term streamflow forecasts (with a lead-time longer than 15 days), have been applied to reservoir operation and water resources management (e.g. [23,25,29,39]).

In addition to forecast precision and lead-time, operation strategies also influence the efficiency of utilizing streamflow forecasts for real-time reservoir operation [4,20,39]. As a common practice, reservoir operation curves, which set a target storage level for each operation period around a year, are adopted as guidelines for real-time reservoir operation as well as for operation planning [18,34]. Since operation curves are determined by historical streamflow records [20,34], they reflect suitable reservoir operation decisions under various historical scenarios rather than real-time streamflow conditions. Thus, even a perfect streamflow forecast cannot improve reservoir operation efficiency when operation curves are used [39]. In many recent studies, reservoir operation curves have been replaced by real-time reservoir optimization and simulation models, which are supposed to provide more flexible and efficient approaches utilizing various streamflow forecast products [8].

One important issue with implementing streamflow forecasts in real-time reservoir operation models is dealing with the uncertainty involved in streamflow forecast products [8,9,26]. Although forecast uncertainty analysis has been one research focus in hydrology (e.g. [17,31,32]), there are comparatively less studies on the effect of forecast uncertainty on real-time reservoir operations [9,27,33]. Deterministic or probabilistic streamflow forecast products are usually treated as *ad hoc* inputs for deterministic or stochastic reservoir operation models. That is to say, a deterministic forecast or a stochastic forecast represented by a number of scenarios is pre-designed for a specific reservoir operation problem for screening test, and no non-generalizable structure of the forecast error is endogenously involved in the operation analysis. Correspondingly, many previous studies on forecast and reservoir operation in the literature adopt a two-component approach, one provides ("recommends") a forecast scenario [3,22,24,28] as input to the other component [23,25,29,39] that dealing with forecast application. In general, such an approach suggests that forecast can always improve reservoir operation efficiency especially under extreme conditions [21].

This study aims at analyzing the effect of forecast uncertainty on real-time reservoir operations. As different forecast products, e.g., deterministic and probabilistic streamflow forecasts, can exert

* Corresponding author. Tel.: +1 (217) 333 4935; fax: +1 (217) 333 0687.
E-mail address: xmcai@illinois.edu (X. Cai).

0309-1708/$ - see front matter © 2011 Elsevier Ltd. All rights reserved.
doi:10.1016/j.advwatres.2011.01.004

different effects on real-time reservoir operation decisions in optimization and simulation models, this study will explicitly simulate the uncertainty in each of the streamflow forecasts examined and assess its effect on real-time reservoir operation decisions. Since the tool for such a purpose does not exist in the hydrologic literature, the Martingale Model of Forecasting Evolution (MMFE) [11,12] used in supply chain management is introduced to quantify real-time streamflow forecast uncertainty and generate deterministic and probabilistic forecast products. Simulations based on standard operation policy (SOP), dynamic programming (DP), and stochastic dynamic programming (SDP) [16,18] are adopted to determine release decisions for a hypothetical reservoir using synthetic streamflow forecasting products.

The rest of the paper is organized as follows. Section 2 provides some background information on streamflow forecasting and forecast uncertainty and introduces the Martingale Model of Forecasting Evolution (MMFE). Section 3 describes the MMFE-based forecast uncertainty analysis in real-time reservoir operation. Section 4 introduces the numerical experiments designed in this study. Section 5 analyzes the results and Section 6 contains the conclusions.

2. Background

In hydrology, there are various indices reflecting the magnitude of streamflow forecast uncertainty (e.g., [24,32]). However, few models illustrate the forecast uncertainty evolution process. This paper adopts MMFE from supply chain management [11,12] to quantify the evolution of the uncertainty of real-time streamflow forecasts as time progresses.

2.1. Streamflow forecast and forecast uncertainty

Both deterministic and probabilistic streamflow forecast products have been applied to real-time reservoir release decision making, as outlined in Fig. 1. Defining q as the actual streamflow and e as the forecast error, the relationship between deterministic streamflow forecast (*DSF*) and q can be interpreted by Eq. (1):

$$DSF = q + e \tag{1}$$

Eq. (1) shows that the forecast uncertainty in *DSF* is characterized by a deterministic forecast error e. Usually, e is assumed to be stochastic and fit a normal distribution (e.g. [2,6,28,29]):

$$e \sim N(0, \sigma^2) \tag{2}$$

where σ^2 denotes the variance of e (i.e., uncertainty level)

Probabilistic streamflow forecasts (*PSF*) can be generated with two approaches. One involves treating the *PSF* as an empirical conditional distribution of forecast uncertainty for a given *DSF* (namely *pseudo-PSF*, denoted as *pPSF* in this study) [6,29]. The premise of *pPSF* is that, since $q = DSF - e$ and $e \sim N(0, \sigma^2)$, the actual streamflow q fits a conditional normal distribution with mean *DSF* and variance σ^2

$$pPSF \sim N(DSF, \sigma^2) = N(q + e, \sigma^2) \tag{3}$$

Eq. (3) shows that the forecast uncertainty in *pPSF* depends on the deterministic forecast error e and the distribution of *pPSF* is conditional to the distribution of e.

The other approach for generating *PSF* takes a more rigorous way to handle forecast uncertainty, which is to characterize the streamflow forecast uncertainty by either the ensemble streamflow forecasting method [5,8,10] or probabilistic streamflow forecasting methods [15,17]. We denote this type of *PSF*, shown in Eq. (4), as a *real-PSF* (*rPSF*) to distinguish it from the *pseudo-PSF* (*pPSF*) presented in Eq. (3). Assuming a normal distribution for forecast uncertainty, *rPSF* can also be characterized with a normal distribution [6,19]:

$$rPSF \sim N(q, \sigma^2) \tag{4}$$

Eq. (4) shows that the forecast uncertainty in *rPSF* is also represented by a probabilistic distribution form. This is different from Eq. (3), which contains a deterministic forecast error term as well as a probabilistic uncertainty term.

This study simplifies forecast uncertainty with the stationary Gaussian distribution assumption and characterizes the single period streamflow forecast uncertainty with σ^2 (the variance of e). In hydrology, σ^2 is closely related to popular hydrologic forecast evaluation criteria, such as the Nash–Sutcliffe efficiency coefficient (*NSE*) and Root Mean Square Error (*RMSE*) [24]. The calculation of *NSE* and *RMSE* are shown in Eqs. (5) and (6), respectively

$$NSE = 1 - \frac{\sum_{i=1}^{M}(f_i - q_i)^2}{\sum_{i=1}^{M}(q_i - \bar{q})^2} \approx 1 - \frac{\sigma^2}{\bar{q} \cdot C_v} \tag{5}$$

$$RMSE = \sqrt{\frac{1}{M}\sum_{i=1}^{M}(f_i - q_i)^2} \approx \sigma \tag{6}$$

where M is the number of samples, C_v is the streamflow coefficient of variation, q_i is the streamflow, and f_i is the streamflow forecast. As can be ascertained from Eqs. (5) and (6), *NSE* measures the comparative level of forecast uncertainty to the streamflow standard deviation and represents the fraction of streamflow variability explained by the forecast while *RMSE* is a direct reflection of the forecast uncertainty itself.

The *PSF* evaluation criteria, e.g., the linear error in probability space (LEPS), the Brier score, mainly depend on the bias and dispersion of the forecasted streamflow distribution, of which σ^2 is an effective statistical indicator [22,24,39].

2.2. Martingale Model of Forecasting Evolution (MMFE)

In streamflow forecasts, denote H as the length of forecast lead time or forecast horizon, within which the streamflow is predictable with an available forecasting method. The streamflow forecasts can be represented by a vector:

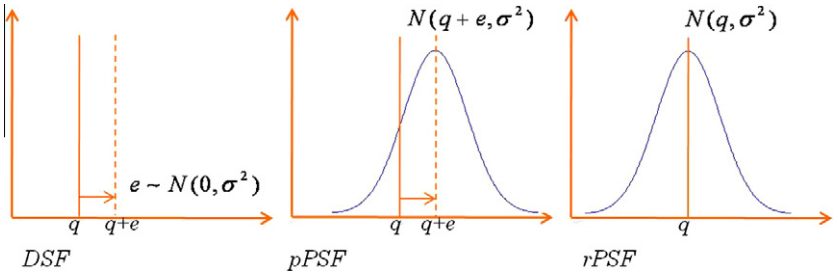

Fig. 1. Schematic of single-period streamflow forecast uncertainty.

$$F_{t,-} = [f_{t,t} \quad f_{1,t+1} \quad f_{t,t+2} \quad \cdots \quad f_{t,t+H}] \tag{7}$$

where $F_{t,-}$ is a vector denoting the forecast sequence made at period t; $f_{t,t+i}$ denotes the period t's forecast for the period $t+i$ streamflow. Denoting $\sigma_{t,t+i}$ as the uncertainty of $f_{t,t+i}$ and assuming (1) stationary forecast uncertainty (i.e., $\sigma_{t,t+i}$ does not change with t) [6,28] and (2) a pre-determined ending time, two important properties of real-time streamflow forecasts hold (as shown in Fig. 2) [19,22,23]:

$$\sigma_{t,t} \leqslant \sigma_{t,t+1} \leqslant \sigma_{t,t+2} \leqslant \cdots \leqslant \sigma_{t,t+H} \tag{8}$$

$$\sigma_{t-H,t} \geqslant \sigma_{t-H+1,t} \geqslant \sigma_{t-H+2,t} \geqslant \cdots \geqslant \sigma_{t,t} \tag{9}$$

Eq. (8) denotes that the uncertainty level of the streamflow forecast increases with the forecast lead time, which is intuitive since the longer the forecast lead time, the less reliable the forecast information is, as shown in the upper part of Fig. 2. Eq. (9) represents a property that indicates the dynamic updating of the real-time streamflow forecast, i.e., when the forecast period moves towards the ending time, information becomes more reliable and the forecast uncertainty level decreases, as shown in the lower part of Fig. 2.

The MMFE model uses a decomposition approach to measure the uncertainty in each of the time periods within the forecast lead time (H):

$$\Delta F_{t,-} = [\Delta f_{t,t} \quad \Delta f_{1,t+1} \quad \Delta f_{t,t+2} \quad \cdots \quad \Delta f_{t,t+H}] \tag{10}$$

where $\Delta F_{t,-}$ is a vector denoting the forecast update made at period t from the forecasts made at period $t-1$ and $\Delta F_{t,t+i}$ is the improvement of streamflow forecast at period $t+i$, and:

$$\Delta f_{t,t+i} = f_{t,t+i} - f_{t-1,t+i} \tag{11}$$

MMFE, which simulates the forecast improvement process, is based on the following four assumptions [12]: (1) $F_{t,-}$ is an unbiased forecast for the future; (2) $\Delta f_{t,t+i}$ is uncorrelated with past forecast updates $\Delta f_{s,s+i} (s < t)$; (3) the forecast update $\Delta f_{t,t+i}$ forms a stationary stochastic process of t; and (4) the forecast update $\Delta f_{t,t+i}$ is normally distributed.

Under MMFE, the total forecast uncertainty can be characterized by the variance–covariance (VCV) matrix of $\Delta F_{t,-}$

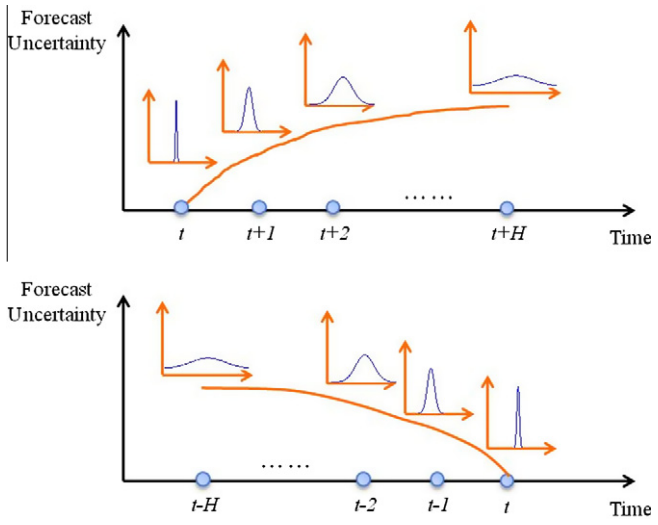

Fig. 2. Schematic of the increase in forecast uncertainty with forecast lead-time.

$$VCV = \begin{bmatrix} \sigma^2_{0,0} & \sigma^2_{0,1} & \cdots & \sigma^2_{0,H} \\ \sigma^2_{1,0} & \sigma^2_{1,1} & \cdots & \sigma^2_{1,H} \\ \vdots & \vdots & \ddots & \vdots \\ \sigma^2_{H,0} & \sigma^2_{H,1} & \cdots & \sigma^2_{H,H} \end{bmatrix}_{(H+1)\times(H+1)} \tag{12}$$

where σ^2_{ij} is the covariance between $\Delta f_{t,t+i}$ and $\Delta f_{t,t+j}$. Denoting $f_{t,t} = q_t$, with Eq. (11), $f_{t-i,t}$ can be expressed by:

$$f_{t-i,t} = q_t - \sum_{j=t-i+1}^{t} \Delta f_{j,t} \tag{13}$$

With Eq. (13) and the second assumption of MMFE, the forecast uncertainty level of $f_{t-i,t}$ can be calculated by:

$$\mathrm{var}(q_t - f_{t-i,t}) = \sum_{j=0}^{i-1} \sigma^2_{j,j} \tag{14}$$

Since $\mathrm{var}(q_t - f_{t,i,t})$ increases with i, MMFE naturally reflects some properties of streamflow forecasts, i.e., increased uncertainty with forecast lead-time and dynamic forecast updates.

It is important to note that MMFE is not a forecast model but rather a framework representing the dynamics of forecast updates [12,14]. Due to its simplicity and effectiveness in illustrating the forecast uncertainty evolution processes, MMFE has been widely applied to operations research for quantifying the economic profits from forecast improvements [12], analyzing the optimality of supply chain management strategies [14,36], determining the safety stock level in supply chain management [30], and supporting restocking decision making under forecast uncertainty [37].

3. MMFE-based streamflow forecast uncertainty analysis

To use MMFE to model the uncertainty of streamflow forecasts, it is necessary to justify its assumptions, i.e. unbiasedness, non inter-period correlation, stationarity, and Gaussian distribution. Real-time streamflow forecasts are based on hydrologic model inputs, such as precipitation, temperature, and soil moisture. These inputs are updated at the beginning of each period with new weather forecasts and hydrologic observations (e.g., streamflow, soil moisture) to improve the preceding streamflow forecast. Since hydrologic model input errors are usually considered to be dominated by random factors rather than structural ones, the assumption of unbiasedness in MMFE (i.e., the structural error is negligible) has been widely adopted in hydrologic studies (e.g. [9,10,29]).

The second assumption may be justified by the hypothetical problem setting in this study. As time moves forward to the prescribed ending period, the forecast lead time decreases and more information becomes available (Fig. 2). At the start of a new period, new information becomes available, which is not available for the previous periods. It is reasonable to assume that this new information is independent from the information that was previously available. Therefore, it can be assumed that the update to the streamflow forecast for a given period is independent of the updates in previous periods.

The third and fourth assumptions imply stationarity and a Gaussian distribution of the uncertainty, respectively, which are common assumptions in hydrologic studies [6,29].

In MMFE, the VCV matrix of the linearly dependent components of $F_{t,-}$ in Eq. (12) plays a central role. Since the VCV matrix is positive semi-definite, it can be decomposed into the product of a matrix multiplied by its transpose through the Cholesky decomposition [1,12], i.e.,

$$VCV = V \cdot V^T \tag{15}$$

Denote $[X_1\ X_2\ \cdots\ X_{H+1}]$ as a vector of $H+1$ independent standard normal variables and transposing it with matrix V^T:

$$[\,Y_1 \quad Y_2 \quad \cdots \quad Y_{H+1}\,] = [\,X_1 \quad X_2 \quad \cdots \quad X_{H+1}\,] \cdot V^T \tag{16}$$

Then, the generated vector of Y consists of normally distributed variables with a variance–covariance matrix equal to their original variance–covariance matrix, $VCV = V \cdot V^T$. Thus, Eq. (16) can be used for generating forecast errors:

$$\begin{bmatrix} \Delta f_{1,1} & \Delta f_{1,2} & \cdots & \Delta f_{1,H+1} \\ \Delta f_{2,2} & \Delta f_{2,3} & \cdots & \Delta f_{2,H+2} \\ \vdots & \vdots & \ddots & \vdots \\ \Delta f_{t,t} & \Delta f_{t,t+1} & \cdots & \Delta f_{t,H+1} \end{bmatrix} = \begin{bmatrix} x_{1,1} & x_{2,1} & \cdots & x_{H+1,1} \\ x_{1,2} & x_{2,2} & \cdots & x_{H+1,2} \\ \vdots & \vdots & \ddots & \vdots \\ x_{1,t} & x_{2,t} & \ldots & x_{H+1,t} \end{bmatrix} \cdot V^T \tag{17}$$

Assuming the actual streamflow sequence is known:

$$Q = [\,q_1 \quad q_2 \quad \cdots \quad q_N\,] \tag{18}$$

The deterministic streamflow forecast error can be expressed by:

$$e_{t-i,t} = q_t - f_{t-i,t} = \sum_{j=H+2-i}^{H+1} \Delta f_{t-H-1+j,t} = \sum_{j=0}^{i-1} \Delta f_{t-j,t} \tag{19}$$

where $e_{t-i,t}$ denotes the forecast error for period t streamflow in the forecast made during period $t-i$. The synthetic *DSF* forecast errors, e.g. $e_{1,5} = \sum_{i=2}^{5} \Delta f_{i,5}$, can then be generated through Eq. (19).

With the second assumption of MMFE, the variance of the forecast error ($e_{t-i,t}$) can be calculated by:

$$\mathrm{var}(e_{t-i,t}) = \sum_{j=0}^{i-1} \sigma_{j,j}^2 \quad (i \geqslant 1) \tag{20}$$

Combining Eqs. 1, 3, 4 with Eqs. (19) and (20), the *DSF*, *pDSF*, and *rDSF* made at period $t-i$ for period t streamflow can be explicitly expressed with the following equations:

$$DSF: \ DSF_{t-i,t} = q_t - e_{t-i,t}\left(e_{t-i,t} \sim N\left(0, \sum_{j=0}^{i-1} \sigma_{j,j}^2\right)\right) \tag{21}$$

$$pPSF: \ pPSF_{t-i,t} \sim N\left(q_t - e_{t-i,t}, \sum_{j=0}^{i-1} \sigma_{j,j}^2\right) \tag{22}$$

$$rPSF: \ rPSF_{t-i,t} \sim N\left(q_t, \sum_{j=0}^{i-1} \sigma_{j,j}^2\right) \tag{23}$$

Thus, using MMFE, *DSF*, *pPSF*, and *rPSF* can be synthetically generated with a common framework. For probabilistic forecasts (*pPSF* and *rPSF*), Eqs. (22) and (23) depict the forecast uncertainty of period t without reflecting the correlation relationship between the uncertain terms expressed in Eqs. (10) and (12). To deal with this concern, this study adopts a scenario-based Monte-Carlo approach for forecast uncertainty analysis [16,35]. Then, with a deterministic or stochastic reservoir operation model (see the Appendix for details), a framework for real-time reservoir release decisions can be established.

It is worthwhile to note that forecast uncertainty and forecast horizon are two important features of streamflow forecast and both can affect reservoir operation using the forecast [33,41], as the forecast can be too uncertain if it is too long (i.e., it cannot reliably reflect inflow conditions) or too short to be applicable for supporting decision making. This study focuses on the effect of forecast uncertainty on real-time reservoir operation while the complicating effect of forecast uncertainty and forecast horizon will be analyzed in future work.

4. Numerical experiments

A hypothetical reservoir system with N operation periods (i.e., studying horizon of the operation problem) is used in this study. In reservoir operation, the forecast lead time H is assumed to be the same as the length of remaining operation periods (i.e., the lead time H is N periods at the beginning, $N-1$ periods when decision moves to next period, and so on). SOP, DP, and SDP models are then used to generate reservoir operation decisions with various synthetic streamflow forecast products. SOP releases water as close to the delivery target as possible, saving only surplus water for future delivery, and it only needs the current period inflow information (Appendix A.1). The formulation of DP and SDP are provided in Appendices A.2 and A.3, respectively.

4.1. The hypothetical reservoir system

Besides forecast uncertainty, the efficiency of reservoir operations can also be affected by reservoir inflow variability, demand change, and reservoir capacity [9,26]. To study these influential factors, the hypothetical reservoir operation model consists of four categories of parameters: forecast uncertainty, reservoir inflow, reservoir capacity, and the objective function.

(1) *Forecast uncertainty:* The forecast error standard deviation σ and the forecast error correlation ρ_{error} are introduced to characterize the streamflow forecast uncertainty [31,32], as shown in Eq. (24). The *VCV* matrix is simplified with the two forecast parameters:

$$\begin{bmatrix} \sigma^2 & \rho_{error}\sigma^2 & \ldots & 0 \\ \rho_{error}\sigma^2 & \rho_{error}\sigma^2 & \ldots & 0 \\ \vdots & \vdots & \ddots & \vdots \\ 0 & 0 & \ldots & \sigma^2 \end{bmatrix}_{(H+1)\times(H+1)} \tag{24}$$

σ represents the magnitude of uncertainty in the forecast. A higher σ value implies a greater forecast uncertainty. ρ_{error} reflects the temporal correlation relationship of the forecast uncertainty. In general, a negative ρ_{error} implies a lower amount of uncertainty in the total inflow, as the overestimated forecast errors are more likely to be balanced by the underestimated forecast errors; meanwhile, a positive ρ_{error} implies a higher degree of uncertainty in the total inflow forecast.

(2) *Reservoir inflow:* The reservoir inflow parameters include the mean, coefficient of variation, and the correlation coefficient of the streamflow, which are denoted as μ, C_v, and ρ_{flow}, respectively. A simplified Thomas–Fiering model [20] is applied to generate the reservoir inflow sequences:

$$q_{t+1} = \mu + \rho_{flow}(q_t - \mu) + \sqrt{1-\rho_{flow}^2}(\mu C_v)\delta \tag{25}$$

In Eq. (25), δ is a standard normal random number. The minimum streamflow is set to 0.4 so that 93% of the generated streamflow sequences can be subsequently used in the MMFE streamflow forecast model when C_v is at its maximum value, i.e., 0.4 (Table 1).

(3) *Reservoir capacity:* The reservoir capacity (S) is represented by the active maximum storage, which is the difference between the maximum and the minimum storage

$$S = S_{\max} - S_{\min} \tag{26}$$

To avoid adverse effects of initial storage and end storage on reservoir operation decisions, the initial storage and end storage are set to half of S.

Table 1
Parameters of the hypothetical reservoir system.

Reservoir components	Parameters symbol	Type	Value range	Base value
Forecast uncertainty	σ	Variable	0.02–0.20	0.10
	ρ_{error}	Variable	−0.50 to 0.50	0
Reservoir inflow	μ	Constant	1	–
	C_v	Variable	0.05–0.40	0.30
	ρ_{flow}	Variable	0.4	–
Reservoir capacity	S	Variable	0.20–5.00	2.00
Reservoir utility	$D_{\min}$	Constant	0.4	–
	$D_{\max}$	Constant	1.2	–

(4) *Objective function:* The objective function is defined as the sum of the single-period reservoir release utility (Eq. (27)) and is maximized in the DP and SDP formulations, in which the reservoir storage and inflow are discretized into intervals with a width of 0.01

$$g_t = \left(\frac{D_t - D_{\min}}{D_{\max} - D_{\min}}\right)^{1/2} \tag{27}$$

where D_t is the beneficial release (excluding the reservoir spill DS_t) at time period t, while $D_{\max}$ and $D_{\min}$ represent the maximum and minimum beneficial releases, respectively. Eq. (27) is concave with a decreasing marginal utility property [7,20,40].

The parameters of the hypothetical reservoir operation model are summarized in Table 1. Each of the impact factors discussed above (as shown in Table 1) is assessed individually, i.e. adjusting the value of a given factor while holding the base values of all other parameters. Table 1 shows the range of values tested for each parameter. It is necessary to note that forecast uncertainty parameters (Eq. (24)) have already been specified with values in Table 1 for this hypothetical case study and the underlying assumption is that MMFE has already been validated before the policy simulation. For real-world application of MMFE, a validation step is needed.

4.2. Reservoir operation strategies

The following generic procedures are used to model the hypothetical reservoir operation problem: (1) time series of streamflow Q during the N operation periods are generated using a flow synthesis model with given reservoir inflow statistics; (2) *DSF*, *pPSF*, and *rPSF* are generated with Q and MMFE using the predefined forecast uncertainty statistics; for *pPSF* and *rPSF*, 500 forecast error scenarios are generated to approximate the streamflow probability and state transition probability [8,16] (see Appendix A.3 for details on the transition probability in the context of SDP); (3) with the synthesized forecast products from (2), optimization models (DP and SDP) and the simulation model based on SOP are employed for reservoir operation analysis. For each parameter test, the numerical experiment is conducted with 100 randomly generated streamflow scenarios, and the mean value and standard deviation of the utility are computed using the 100 samples.

Decision horizon (DH, how long the generated decision is implemented), forecast horizon (FH, how long the inflow can be predicted), and operation horizon (OH, how long the reservoir operation is targeted) are important issues in reservoir operation (also see [41]). In our study, DH is set as 1 and FH is assumed to be the same as the length of OH (i.e., the lead time H is N periods at the beginning, $N-1$ periods when decision moves to next period, and so on). The following procedures are undertaken for the modeling exercise: (1) reservoir operation decision is determined for each period with the streamflow forecast provided up to the end of the operation periods; (2) for the generated decision sequence (Eqs. (A3) and (A4)), only the current period decision is treated as final; (3) decisions in future time periods will be updated period by period, i.e., at the beginning of the next period, the reservoir state is updated with inflow and release, and new release decision is made with updated forecast (i.e., rolling horizon decision making, see Fig. 3). This process is repeated from period 1 to N (N is set as 6 in this study).

This study undertakes a finite horizon specified with the ending storage, which is set equal to the initial storage for this theoretical study. Five operation scenarios, shown in the last column of Fig. 4, are examined. The optimization models of dynamic programming (DP) and stochastic dynamic programming (SDP) are utilized to generate the operation decisions with the streamflow forecast. The perfect forecast, Q, and *DSF* are implemented through DP while the probabilistic forecast scenarios (*pPSF* and *rPSF*) are implemented through SDP. These results are compared to a simulation model of standard operation policy (SOP) using Q. A brief summary of reservoir operation models is provided in the Appendix.

5. Result analysis

The effect of streamflow forecast uncertainty on real-time reservoir operation is analyzed with reservoir operation models DP, SDP, and SOP. In the context of forecast uncertainty analysis, the effect of streamflow variability and reservoir capacity are also assessed under a pre-specified forecast uncertainty level, as shown in Table 1.

5.1. The role of forecast uncertainty for reservoir operation

With the base parameter values in Table 1, effects of different values of σ and ρ_{error} are assessed. Figs. 5 and 6 show the effect of σ and ρ_{error} on the utility level of the reservoir operation, respectively. The mean value and standard deviation of the reservoir operation improvement (in terms of utility increase) with deterministic forecasts (Q-DP and *DSF*-DP) and probabilistic forecasts

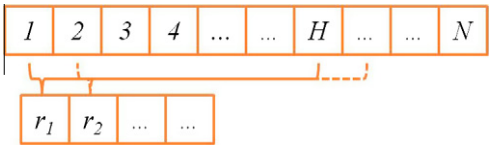

Fig. 3. Schematic of rolling horizon decision making in reservoir operation (H is assumed equal to N in this study).

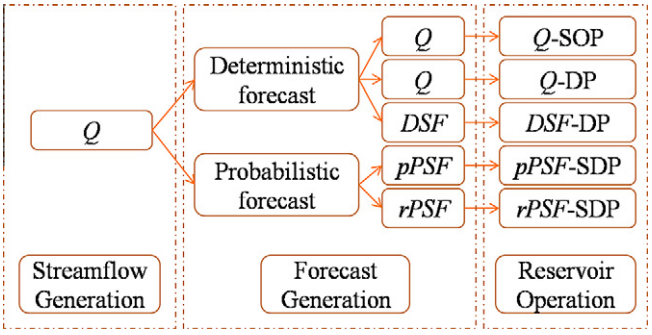

Fig. 4. Procedures of modeling exercise for testing the various forecasts with reservoir operation models.

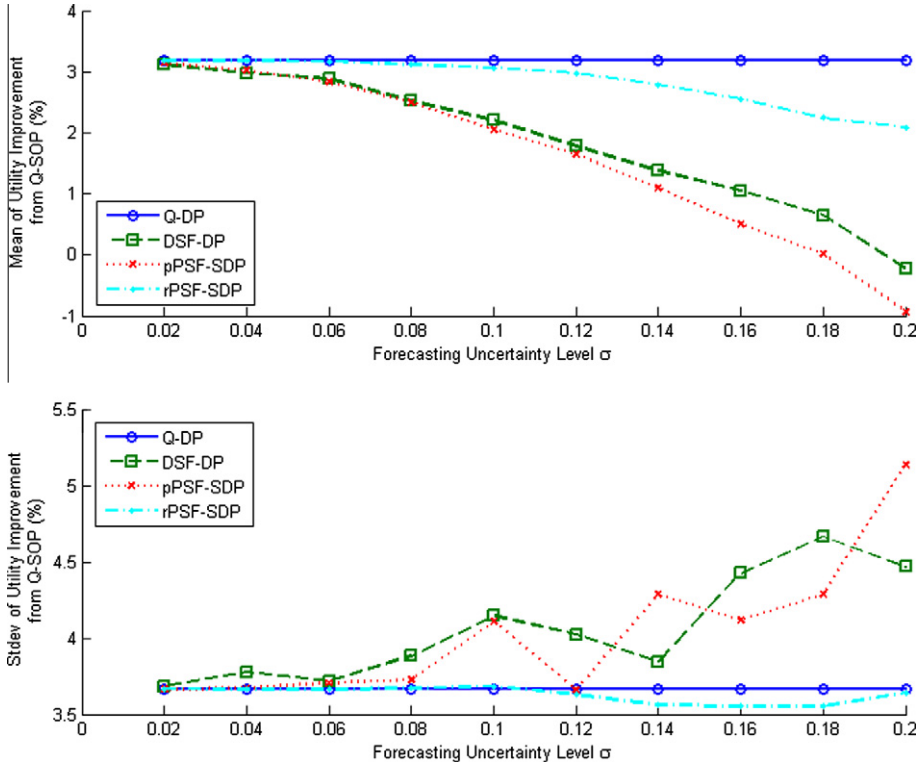

Fig. 5. Relationship between reservoir operation efficiency improvement from SOP and streamflow forecast uncertainty level.

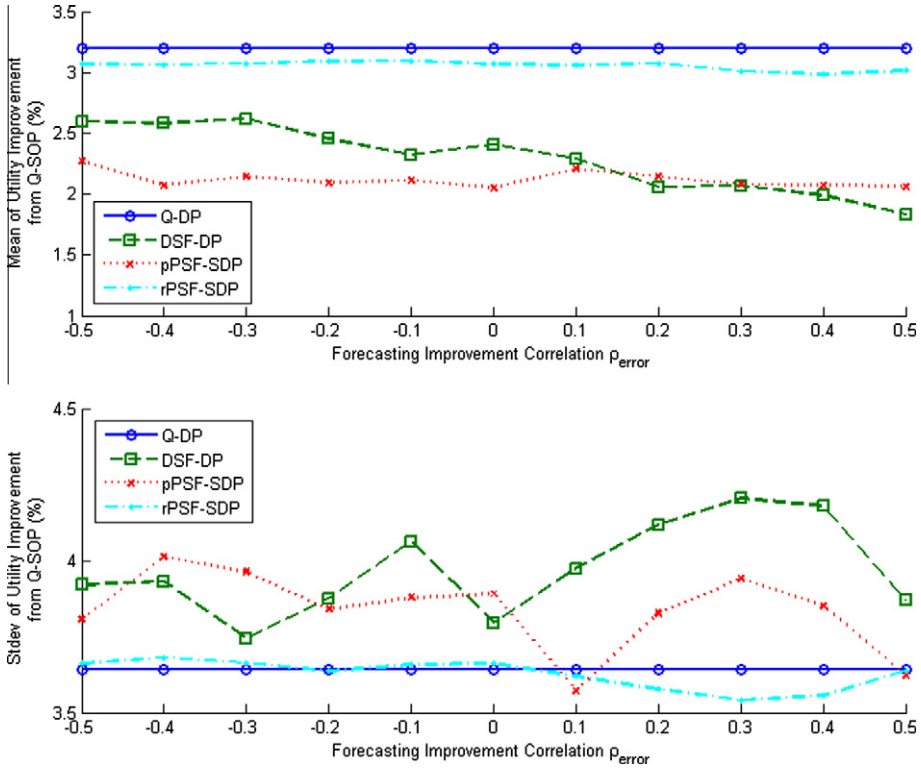

Fig. 6. Relationship between reservoir operation efficiency improvement from SOP and correlation of forecast errors.

(*pPSF*-SDP and *rPSF*-SDP) from *Q*-SOP are compared in Fig. 5. As can be seen from the upper part of Fig. 5, a threshold level exists in the *rPSF*-SDP performance. With a medium uncertainty level $\sigma < 0.1$ ($\sigma = 0.1$ is about one third of the streamflow standard deviation $\mu C_v = 0.3$), the operation of *rPSF*-SDP is similar to *Q*-DP (i.e., the optimal reservoir release decision) in terms of the mean utility

improvement from *Q*-SOP. Beyond this uncertainty level $\sigma > 0.1$, *rPSF*-SDP has a decreasing trend with the increase of forecast uncertainty level. The performances of *DSF*-DP and *pPSF*-SDP are similar with a declining trend in the forecast uncertainty level. In terms of the standard deviation of the utility improvement, *Q*-DP and *rPSF*-SDP both exhibit a lower variation while *DSF*-DP and *pPSF*-SDP show a higher variation. In general, *rPSF* performs superiorly to *pPSF* in terms of improving the real-time reservoir operation, which suggests that merely carrying out an empirical uncertainty analysis based on *DSF* is not as efficient as an ensemble streamflow forecast.

Fig. 6 shows the reservoir performances under different forecast uncertainty correlations varying between −0.5 and 0.5. As with the impact of uncertainty levels (Fig. 5), both *Q*-DP and *rPSF*-SDP perform similarly, which further illustrates the robustness of reservoir operation under *rPSF* with respect to uncertainty correlation. *DSF*-DP and *pPSF*-SDP both show worse performances than *Q*-DP and *rPSF*-SDP. However, the performance of *pPSF*-SDP is more stable with different ρ_{error} levels, while the mean performance of *DSF*-DP shows a slightly declining trend with ρ_{error}, as shown in Fig. 6.

One characteristic of the probabilistic streamflow forecast is its explicit probabilistic representation of future low and high flow conditions, which is important in decision risk analysis. In reservoir operation practice, hedging, which means slightly reducing the current water supply to mitigate future water shortages, is an important real-time reservoir operation practice [7,40]. As forecast uncertainty increases, it becomes more beneficial to adopt hedging to avoid large shortages [40]. Comparing the first period reservoir release reduction under *DSF*-DP, *pPSF*-SDP, and *rPSF*-SDP to that under the perfect forecast *Q*-DP (i.e., the optimal reservoir operation without forecast uncertainty), the hedging effects of both *pPSF*-SDP and *rPSF*-SDP exhibit an increasing trend with the increase of the uncertainty level. On the other hand, *DSF-DP* shows no significant hedging effect (as shown in Fig. 7), which illustrates the effectiveness of adopting probabilistic streamflow forecasts to represent the future risks. Meanwhile, although the hedging trends under *pPSF* and *rPSF* are similar, there are differences between *pPSF*-SDP and *rPSF*-SDP in terms of utility improvement from *Q*-SOP (as shown in Figs. 5 and 6). The reason can be that the *pPSF*-SDP operation hedges against both the deterministic forecast error and the random forecast uncertainty. Since the magnitude of the deterministic forecast error is approximate to that of the forecast uncertainty (denoted by the standard deviation of the deterministic forecast error, as shown in Eqs. (1)–(3)), the benefit of hedging is not as significant in *pPSF*-SDP as *rPSF*-SDP. Also, the hedging effect of *pPSF*-SDP tends to be more variable than that of *rPSF*-SDP.

5.2. Effect of streamflow variability

A reservoir is built to regulate natural streamflow variability and to maintain a reliable utility from natural streamflow [18,20]. The coefficient of variation C_v, which is defined as the ratio of the streamflow standard deviation over the mean value, is commonly used to characterize the inter-period streamflow variability. Fig. 8 displays the effect of C_v on reservoir operation performances under the various forms of forecast uncertainty.

Fig. 8 illustrates that, with the increase of C_v, the utility improvements relative to SOP under all the optimized solutions with deterministic or probabilistic forecasts tend to increase. This generally implies that the more variable the streamflow is, the more valuable the forecast is for improving reservoir operation efficiency. Meanwhile, reservoir operation under *rPSF* shows robustness with a high uncertainty level (comparable to the natural variability), for example, when $C_v = 0.1$ (i.e., the forecast uncertainty is comparable to the streamflow variability σ), about 50% of the reservoir operations under *DSF*-DP and about 80% of the reservoir operations under *pPSF*-SDP are inferior to *Q*-SOP, while *rPSF*-SDP shows a performance similar to *Q*-DP and better than *DSF*-DP.

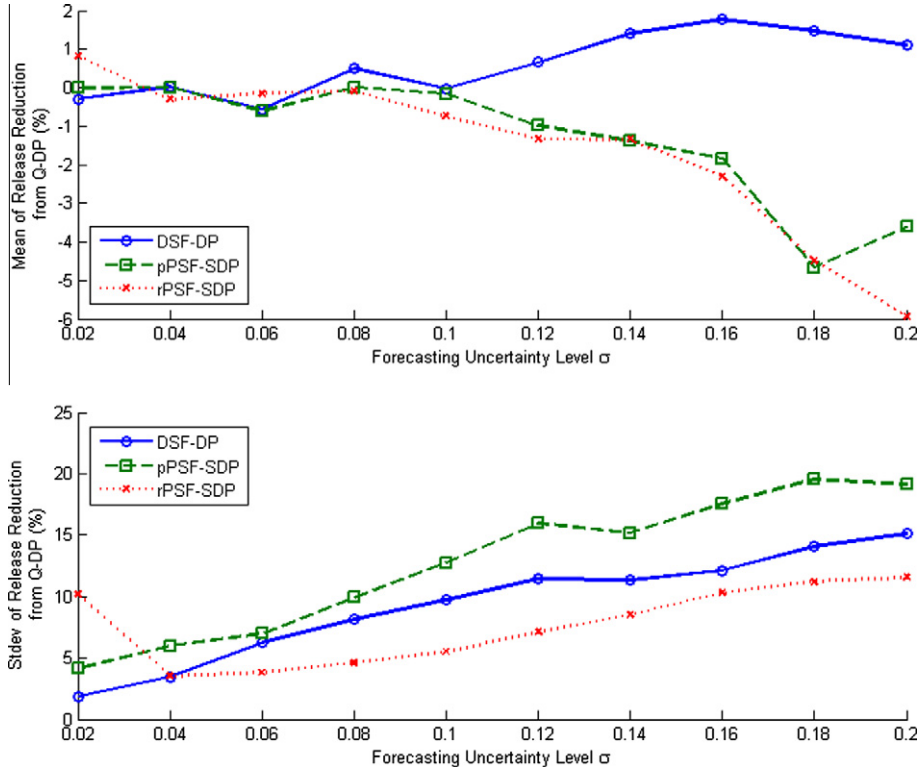

Fig. 7. Hedging effects resulting from application of streamflow forecasts to reservoir operation.

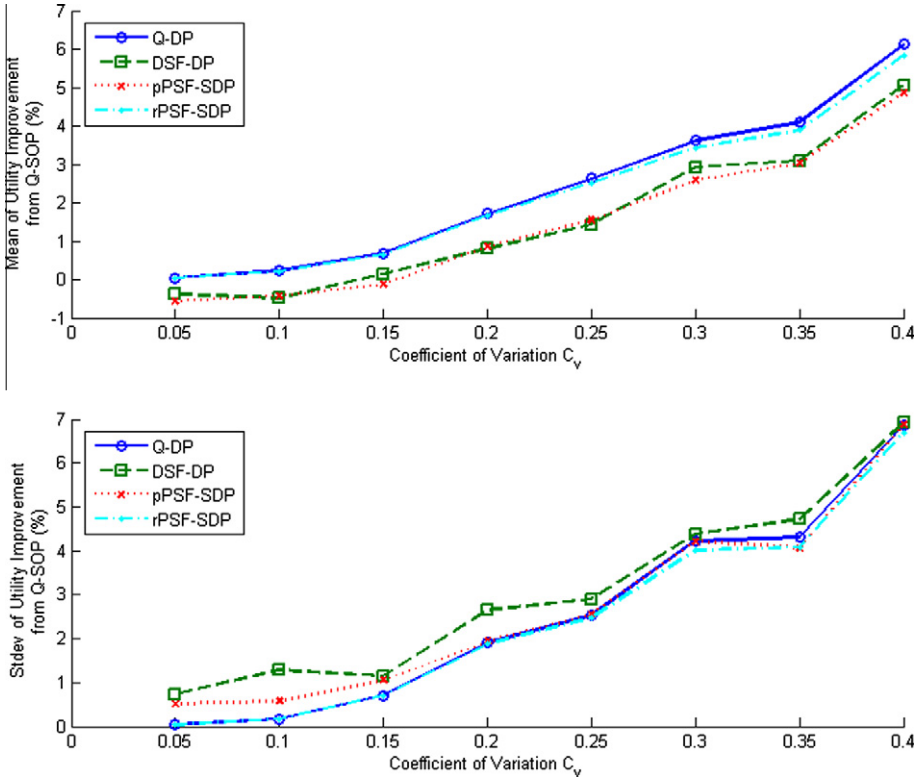

Fig. 8. Effect of streamflow variability on the application of streamflow forecasts to reservoir operation.

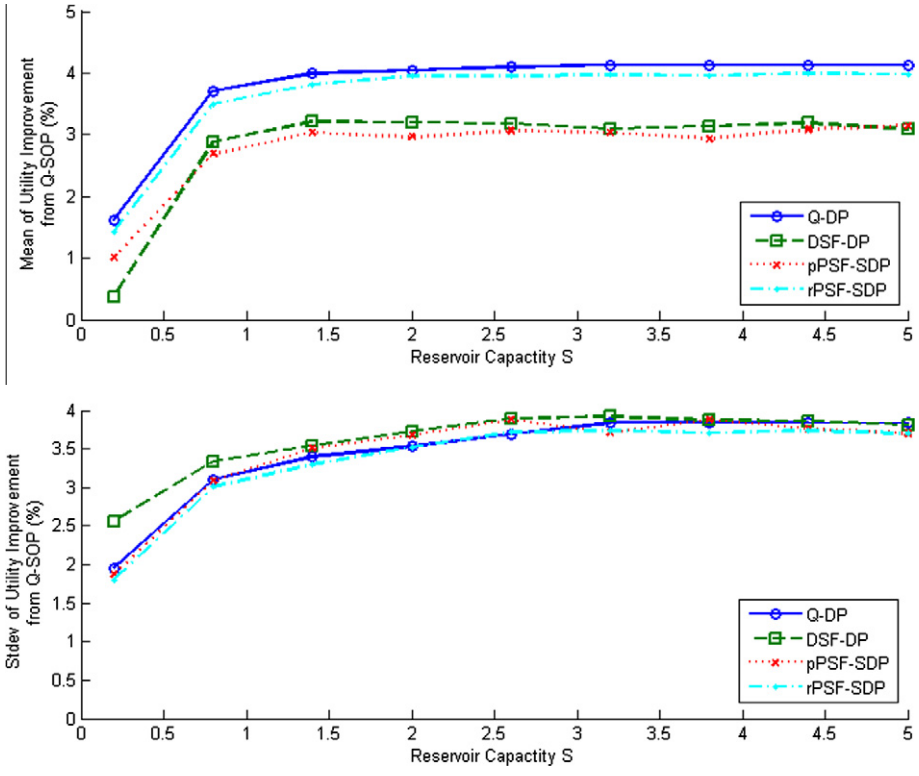

Fig. 9. Effect of reservoir capacity on the application of streamflow forecasts to reservoir operation.

5.3. Effect of reservoir capacity

The effect of reservoir capacity is studied by varying reservoir capacity S from 20% to 500% of the mean inflow (μ in Eq. (25)), of which the results are shown in Fig. 9. With respect to mean utility improvement, the *DSF*-DP and *rPSF*-SDP perform similarly. *DSF*-DP performs more poorly than *pPSF*-SDP when the storage is small, and gradually improves and approaches the performance of *pPSF*-

SDP as the reservoir storage becomes larger. This is different from the above comparisons between *DSF*-DP and *pPSF*-SDP, where the *DSF*-DP performs similarly to *pPSF*-SDP under various forecast uncertainty and streamflow variability levels. Note that *pPSF* differs from *DSF* because it includes an empirical uncertainty analysis that addresses the risk induced by forecast error. Thus the poor performance of *DSF*-DP compared to *pPSF*-SDP when the reservoir storage is small implies that small reservoirs are more sensitive to forecast uncertainties [9,13,15]. Standard deviation values of utility improvements show a similar performance with the increase of reservoir storage, except that the *DSF*-DP has a larger standard deviation when the reservoir storage is small. This also suggests that the *DSF*-guided reservoir operation is vulnerable to forecast errors when the reservoir is small.

6. Conclusions

Streamflow forecast uncertainty plays an important role in reservoir operation, but the effects of forecast uncertainty on reservoir operation have yet to be thoroughly addressed in a unifying framework. Rather than treating the forecast products as *ad hoc* inputs to reservoir operation models, this study provides a method to characterize the forecast uncertainty evolution and explicitly assess the effect of streamflow forecast uncertainty on real-time reservoir operation. The Martingale Model of Forecast Evolution (MMFE) is introduced to synthetically generate deterministic and probabilistic streamflow forecasts through explicit representations of forecast uncertainty under various scenarios. A simulation model based on SOP with a perfect forecast, two DP models with a perfect forecast and *DSF*, respectively, and two SDP models with *pPSF* and *rPSF*, respectively, are employed to analyze the impact of forecast information on reservoir operation.

The hypothetical case study shows that reservoir operation efficiency decreases as forecast uncertainty increases, while these effects also depend on the type of forecast product being used. In general, the reservoir operation under *rPSF* is near-optimal and comparable to the optimized reservoir operation decision obtained with a perfect forecast. The reservoir operations under *DSF* and *pPSF* are similar but not as efficient as they are under *rPSF*. Thus, ensemble and probabilistic streamflow forecasts, which are widely used in stochastic hydrologic modeling, have the potential to improve real-time reservoir operation. Moreover, the effect of forecast uncertainty is complicated by streamflow variability and reservoir storage capacity. As the streamflow variability increases, the reservoir system is subject to more frequent extreme flow (both low-flow and high-flow) threats and streamflow forecasts are more valuable for guiding reservoir operations. The results also show that reservoirs with a smaller storage capacity are more sensitive to forecast errors and, as a result, it is more valuable to consider the forecast uncertainty in the operation of these reservoirs. In summary, the simulations presented in this study show the significance of considering deterministic and probabilistic forecast uncertainty in real-time reservoir operation and illustrate the promising application of ensemble and probabilistic streamflow forecasts.

This study simulates the forecast uncertainty using a conceptual model, MMFE, which decomposes the total forecast uncertainty into the uncertainties of individual single periods and assumes unbiasedness, non inter-period correlation, stationarity, and the Gaussian distribution of the single period uncertainty. It should be noted that the forecast simulated in this study is simplified compared to the real-world situation, which can be complicated by correlated, heteroscedastic, and non-Gaussian features. While only one parameter needs to be simulated in MMFE with a Gaussian distribution, more than one parameter with a non-Gaussian distribution must be handled in MMFE. This will make the analysis complex with both conceptual and computational issues to resolve, although the general procedures of MMFE are applicable to a non-Gaussian case. For example, the correlation among the multiple parameters may be considered; the assumptions for forecast improvement (Eq. (10)) may need to be adjusted. On the other hand, studies on hydrologic forecast errors that attempt to remove the stationary and/or Gaussian assumptions are undergoing [26,31,32], which is expected to provide more scientific support to the use of forecast for real-world reservoir operations.

Acknowledgements

This research was partially supported by the China Overseas Scholarship Foundation, the National Natural Science Foundation of China (Project No. 50928901) and the US National Aeronautics and Space Administration (NASA) grant (Project No. NNX08AL94G). The authors are grateful for the numerous helpful suggestions from Dr. Mohamad Hejazi on the early versions of this paper.

Appendix A. Reservoir operation models

A.1. Standard operation policy (SOP)

SOP releases water as close to the delivery target ($D_{\max}$) as possible and saves only surplus water for future delivery [40]:

$$D_t = \begin{cases} S_t + q_t & (S_t + q_t \leqslant D_{\max}) \\ D_{\max} & (S_t + q_t > D_{\max}) \end{cases} \tag{A1}$$

The spill in SOP is determined as follows:

$$DS_t = \begin{cases} 0 & (S_t + q_t - D_t \leqslant S_{\max}) \\ S_t + q_t - D_t - S_{\max} & (S_t + q_t - D_t > S_{\max}) \end{cases} \tag{A2}$$

A.2. Dynamic programming (DP)

Denoting i and j as the index of discretized reservoir storage, t as the index of time period, DP employs reservoir storage $S_{t,i}$ for the state variable and the recursive function is as follows [18,38]:

$$\begin{cases} G_t(S_{t,i}) = \max\limits_j [g_t(D_t) + G_{t+1}(S_{t+1,j})] \\ S_{t,i} + x_t - (D_t + DS_t) = S_{t+1,j} \end{cases} \tag{A3}$$

In Eq. (A3), x_t is the deterministic streamflow forecast (Eq. (1)), $g_t(\,)$ and $G_t(\,)$ are the single-period and maximum cumulative utility function respectively.

A.3. Stochastic Dynamic Optimization (SDP)

Denoting i and j as the index of discretized reservoir storage, p and q the index of discretized inflow, and t the index of time period, SDP employs both $x_{t,p}$ and $S_{t,i}$ for the state variables and the recursive function can be written as follows:

$$\begin{cases} G_t(S_{t,i}, x_{t,p}) = \max\limits_j \{g_t(D_t) + \sum\limits_q [ST_t(p,q) G_{t+1}(S_{t+1,j}, x_{t+1,q})]\} \\ S_{t,i} + x_{t,p} - (D_t + DS_t) = S_{t+1,j} \end{cases} \tag{A4}$$

In Eq. (A4), $ST_t(p,q)$ represents the inflow state transition probability from p in period t to q in the following period. Denote $PX_t(p)$ as the probability of inflow is p at period t, then

$$PX_{t+1}(q) = \sum_p PX_t(p) ST_t(p,q) \tag{A5}$$

If the temporal independence of forecast uncertainty is ignored, $ST_t(p,q)$ can be simplified as $PX_{t+1}(q)$, but this can underestimate the risk of consecutive high/low flow. Thus, $ST_t(p,q)$ and Eq. (A4) is adopted for decision making with *pPSF* and *rPSF*.

References

[1] Arteaga F, Ferrer A. How to simulate normal data sets with the desired correlation structure. Chemom Intell Lab Syst 2010;101:38–42.
[2] Baker KR. An experimental study of the effectiveness of rolling schedules in production planning. Decision Sci 1977;8:19–27.
[3] Carpenter TM, Georgakakos KP. Assessment of Folsom Lake response to historical and potential future climate scenarios: 1. Forecasting. J Hydrol 2001;249:148–75.
[4] Celeste AB, Billib M. Evaluation of stochastic reservoir operation optimization models. Adv Water Resour 2009;32:1429–43.
[5] Cloke HL, Pappenberger F. Ensemble flood forecasting: a review. J Hydrol 2009;375:613–26.
[6] Datta B, Burges SJ. Short-term, single, multi-purpose reservoir operation – importance of loss functions and forecast errors. Water Resour Res 1984;20:1167–76.
[7] Draper AJ, Lund JR. Optimal hedging and carryover storage value. J Water Res Plan Manage – ASCE 2004;130:83–7.
[8] Faber BA, Stedinger JR. Reservoir optimization using sampling SDP with ensemble streamflow prediction (ESP) forecasts. J Hydrol 2001;249:113–33.
[9] Georgakakos KP, Graham NE. Potential benefits of seasonal inflow prediction uncertainty for reservoir release decisions. J Appl Meteorol Climatol 2008;47:1297–321.
[10] Georgakakos KP, Seo DJ, Gupta H, Schaake J, Butts MB. Towards the characterization of streamflow simulation uncertainty through multimodel ensembles. J Hydrol 2004;298:222–41.
[11] Graves SC. A tactical planning-model for a job shop. Oper Res 1986;34:522–33.
[12] Heath DC, Jackson PL. Modeling the evolution of demand forecasts with application to safety stock analysis in production distribution systems. IIE Trans 1984;26:17–30.
[13] Hejazi MI, Cai XM, Ruddell BL. The role of hydrologic information in reservoir operation – learning from historical releases. Adv Water Resour 2008;31:1636–50.
[14] Iida T, Zipkin PH. Approximate solutions of a dynamic forecast-inventory model. M&SOM 2006;8:407–25.
[15] Karamouz M, Houck MH. Comparison of stochastic and deterministic dynamic-programming for reservoir operating rule generation. Water Resour Bull 1987;23:1–9.
[16] Kelman J, Stedinger JR, Cooper A, Hsu E, Yuan SQ. Sampling stochastic dynamic-programming applied to reservoir operation. Water Resour Res 1990;26:447–54.
[17] Krzysztofowicz R. Bayesian theory of probabilistic forecasting via deterministic hydrologic model. Water Resour Res 1999;35:2739–50.
[18] Labadie JW. Optimal operation of multireservoir systems: state-of-the-art review. J Water Res Plan Manage – ASCE 2004;130:93–111.
[19] Lettenmaier DP. Synthetic streamflow forecast generation. J Hydraul Eng – ASCE 1984;110:277–89.
[20] Loucks DP, Stedinger JR, Haith DA. Water resources systems planning and analysis. Englewood Cliffs, NJ: Prentice-Hall, Inc.; 1981.
[21] Martinez L, Soares S. Comparison between closed-loop and partial open-loop feedback control policies in long term hydrothermal scheduling. IEEE Trans Power Syst 2002;17(2):330–6.
[22] Maurer EP, Lettenmaier DP. Predictability of seasonal runoff in the Mississippi River basin. J Geophys Res – Atmos 2003;108(D16).
[23] Maurer EP, Lettenmaier DP. Potential effects of long-lead hydrologic predictability on Missouri River main-stem reservoirs. J Climate 2004;17(1):174–86.
[24] McCollor D, Stull R. Hydrometeorological short-range ensemble forecasts in complex terrain. Part I: Meteorological evaluation. Weather Forecast 2008;23(4):533–56.
[25] McCollor D, Stull R. Hydrometeorological short-range ensemble forecasts in complex terrain. Part II: Economic evaluation. Weather Forecast 2008;23(4):557–74.
[26] Graham NE, Georgakakos KP. Toward understanding the value of climate information for multiobjective reservoir management under present and future climate and demand scenarios. J Appl Meteorol Climatol 2010;49(4):557–73.
[27] Pianosi F, Soncini-Sessa R. Real-time management of a multipurpose water reservoir with a heteroscedastic inflow model. Water Resour Res; 45:W10430. doi:10.1029/2008WR007335.
[28] Sankarasubramanian A, Lall U, Devineni N, Espinueva S. The role of monthly updated climate forecasts in improving intraseasonal water allocation. J Appl Meteorol Climatol 2009;48(7):1464–82.
[29] Sankarasubramanian A, Lall U, Espinueva S. Role of retrospective forecasts of GCMs forced with persisted SST anomalies in operational streamflow forecasts development. J Hydrometeorol 2009;9(2):212–27.
[30] Schoenmeyr T, Graves SC. Strategic safety stocks in supply chains with evolving forecasts. M&SOM 2009;11(4):657–73.
[31] Schaefli B, Talamba DB, Musy A. Quantifying hydrological modeling errors through a mixture of normal distributions. Journal of Hydrology 2007;332:303–15.
[32] Schoups G, Vrugt JA. A formal likelihood function for parameter and predictive inference of hydrologic models with correlated, heteroscedatic, and non-Gaussian errors. Water Resour Res; 46:W10531. doi:10.1029/2009WR008933.
[33] Simonovic SP, Burn DH. An improved methodology for short-term operation of a single multipurpose reservoir. Water Resour Res 1989;25(1):1–8.
[34] Turgeon A. Stochastic optimization of multireservoir operation: the optimal reservoir trajectory approach. Water Resour Res; 43:W05420. doi:10.1029/2005WR004619.
[35] Vicuna S, Dracup JA, Lund JR, Dale LL, Maurer EP. Basin-scale water system operations with uncertain future climate conditions: methodology and case studies. Water Resour Res 2010;46:W04505. doi:10.1029/2009WR007838.
[36] Wang T, Toktay BL. Inventory management with advance demand information and flexible delivery. Manage Sci 2008;54:716–32.
[37] Wang YM, Tomlin B. To wait or not to wait: optimal ordering under lead time uncertainty and forecast updating. Nav Res Log 2009;56:766–79.
[38] Yakowitz S. Dynamic-programming applications in water-resources. Water Resour Res 1982;18:673–96.
[39] Yao H, Georgakakos A. Assessment of Folsom Lake response to historical and potential future climate scenarios. 2. Reservoir management. J Hydrol 2001;249:176–96.
[40] You JY, Cai XM. Hedging rule for reservoir operations: 1. A theoretical analysis. Water Resour Res; 44:W01415. doi:10.1029/2006WR005481.
[41] You JY, Cai XM. Determining forecast and decision horizons for reservoir operations under hedging policies. Water Resour Res; 44:W11430. doi:10.1029/2008WR006978.